UNITED STATES DEPARTMENT OF AGRICULTURE
SOIL CONSERVATION SERVICE
WASHINGTON, D. C.
H. H. BENNETT, CHIEF

AN ANALYSIS OF SEDIMENT TRANSPORTATION IN THE LIGHT OF FLUID TURBULENCE

By

Hunter Rouse

Cooperative Laboratory
California Institute of Technology

Sedimentation Division
SCS-TP-25
July 1939

UNITED STATES DEPARTMENT OF AGRICULTURE
SOIL CONSERVATION SERVICE
Washington, D. C.
H. H. Bennett, Chief

AN ANALYSIS OF SEDIMENT TRANSPORTATION IN THE LIGHT OF FLUID TURBULENCE

By

Hunter Rouse

Cooperative Laboratory
California Institute of Technology

Presented before the Waterways Division
at the Annual Meeting of the
American Society of Civil Engineers
New York City, January 19, 1939.

Sedimentation Division

AN ANALYSIS OF SEDIMENT TRANSPORTATION IN THE LIGHT OF FLUID TURBULENCE

By Hunter Rouse[1]

Method of Approach

Sediment transportation, like many another engineering problem, has long been studied in a purely empirical manner in the attempt to develop useful working rules from a limited supply of measured data. Since formulas for predicting the sediment load of a stream are generally based upon past records for similar types of flow, they can be depended upon to yield satisfactory results only within this range of flow conditions. Nevertheless, any empirical formula is almost certain to be extrapolated far beyond its limit of validity--a procedure leading sooner or later to serious error, for it is practically impossible to obtain and evaluate enough field measurements to establish empirically a truly general transport law.

Purely rational methods, on the other hand, are even less likely to provide an ultimate solution, owing to the many simplifications which are necessary before a rigorous mathematical treatment becomes possible. In other words, neither mathematical tools nor physical understanding of their use can be considered sufficiently far advanced to cope with so intricate a problem at the present time.

In recent years, however, considerable progress in hydraulic research has resulted from methods that are a "healthy" combination of the empirical and the rational, the process of physical analysis being closely correlated with experimental observation. That is, after eliminating those factors which observation has shown to be of minor importance, the essential features of the problem are analyzed in as rational a manner as possible. All conclusions are then subjected to a thorough experimental check, the number of data necessary to the purely empirical approach having been greatly reduced through systematic organization of the variables.

---

[1]Associate Hydraulic Engineer, Sedimentation Division, Soil Conservation Service, U. S. Department of Agriculture (cooperative laboratory at the California Institute of Technology, Pasadena, Calif.)

The practicability of this method is evidenced by the progress which it has made possible in the study of fluid turbulence. Although turbulent flow is still not fully understood, means have been found of estimating the velocity distribution and resistance of flow along smooth and rough boundaries in a manner which has possibilities of very broad application. Not only should such methods prove equally useful in the study of sediment transportation, but existing knowledge of turbulent flow should have direct bearing upon this problem. Indeed, the analysis of sediment suspension purely as a phenomenon of fluid turbulence has already attracted considerable attention.

For a number of reasons, the movement of bed load and the movement of suspended load have always been treated as two unrelated phases of the transport problem. In many localities the sediment load of streams is for the most part too coarse to be carried in suspension, and the problem remains one of bed load alone. In other instances the task of the engineer has been to keep a watercourse open to traffic, and the regulation of the coarser material moving near the bed has been his sole concern. These circumstances, in turn, have focused attention upon the hydraulic river model, in which only the bed load can be properly simulated. As a matter of fact, not until recent years has suspended material begun to receive its share of attention because of the growing importance of silt control in reservoirs and irrigation projects.

While a fair degree of success has accompanied the study of bed load by purely empirical methods, these have not seemed to lend themselves so readily to the more advanced stage of sediment suspension. On the other hand, though the suspension of sediment by turbulence is apparently more susceptible to rational analysis, the treatment of suspended load as a completely independent problem has proved to be impossible, for the turbulence of the flow and the amount of material carried into suspension are both governed by conditions in the bed region. It is evident, therefore, that an analysis of the sediment problem as a whole will first become possible when bed load and suspended load can be expressed as functions of the same flow parameters.

Turbulence and Bed Load

Although flow boundaries may be loosely classed as either rough or smooth, boundary roughness is actually a relative matter. It has been found expedient in the study of flow through pipes (9)[2]

---

[2]Numbers in parentheses refer to Literature Cited, pp. 24-25.

to define relative roughness as the ratio of a characteristic roughness height to the radius or diameter of the pipe; even then, however, a pipe of a given relative roughness may be effectively smooth at one Reynolds number, and rough at another. While the relative roughness of the pipe and the Reynolds number of the flow are the two parameters which determine the type of flow to be expected, considerable light is thrown on the problem by introducing another type of relative roughness--the absolute roughness of the boundary in its ratio to the thickness of the zone of laminar flow along the pipe wall.

Within the thin laminar layer at a very smooth boundary (shown at greatly exaggerated scale in fig. 1), the velocity increases so rapidly from zero to that of the surrounding turbulent flow that it may be assumed to vary with the first power of the distance from the boundary surface. Thus, in terms of the intensity of boundary shear and the dynamic viscosity of the fluid[3]

$$v = \frac{\tau_o y}{\mu} \tag{1}$$

or, introducing the density and kinematic viscosity, and rewriting in dimensionless form

$$\frac{v}{\sqrt{\tau_o/\rho}} = \sqrt{\frac{\tau_o}{\rho}}\,\frac{y}{\nu} \tag{2}$$

The factor $\sqrt{\tau_o/\rho}$ has the dimension of a velocity, and is commonly known as the "friction velocity." It is proportional to the mean velocity of flow and the square root of the resistance coefficient,

$$\sqrt{\tau_o/\rho} = V\sqrt{f/8}$$

In the zone of fully developed turbulence in very smooth pipes, velocity measurements follow the analytical relationship

$$\frac{v}{\sqrt{\tau_o/\rho}} = 5.5 + 5.75 \log\left(\sqrt{\frac{\tau_o}{\rho}}\,\frac{y}{\nu}\right) \tag{3}$$

If the thickness of the boundary layer is arbitrarily defined as the intersection of the velocity curves of equations 2 and 3 (fig. 1), it will be found that

$$\delta = \frac{11.6\,\nu}{\sqrt{\tau_o/\rho}} \tag{4}$$

---

[3]For table of symbols and their significance refer to Tabulation of Symbols on pp. 22-23.

whereupon equation 3 may be rewritten in terms of boundary-layer thickness:

$$\frac{v}{\sqrt{\tau_o/\rho}} = 11.6 + 5.75 \log \frac{y}{\delta} \tag{5}$$

Nikuradse (6), who determined the constants of equation 3, extended his research to pipes which had been artificially roughened by cementing sand grains on the inner surface. Using the grain diameter, d , as a measure of absolute roughness, k , the velocity distribution in such pipes was found to be expressible in the form

$$\frac{v}{\sqrt{\tau_o/\rho}} = 5.75 \log \frac{y}{d} + \varphi\left(\sqrt{\frac{\tau_o}{\rho}}\ \frac{d}{\nu}\right) \tag{6}$$

in which the function $\varphi\left(\sqrt{\tau_o/\rho}\ \frac{d}{\nu}\right)$ will be seen to be equivalent to $\varphi'(d/\delta)$. In other words,

$$\frac{v}{\sqrt{\tau_o/\rho}} - 5.75 \log \frac{y}{d} = \varphi'\left(\frac{d}{\delta}\right) \tag{7}$$

A plot of measured data in the form $v\sqrt{\tau_o/\rho} - 5.75 \log y/d$ versus d/δ is shown in figure 2; the ratio of absolute roughness to boundary-layer thickness is seen to be of decided importance.

For very low values of d/δ , the wall irregularities are fully enclosed by the laminar layer (fig. 3a), and the flow is then effectively the same as that through an absolutely smooth pipe. Equation 5, for smooth pipes, should describe such motion when rewritten in terms of roughness parameters. Subtracting $5.75 \log y/d$ from both sides of this expression, it will be seen that

$$\frac{v}{\sqrt{\tau_o/\rho}} - 5.75 \log \frac{y}{d} = 5.75 \log \frac{d}{\delta} + 11.6 \tag{8}$$

which is the equation of the sloping line at the left of figure 2, approached asymptotically by the measured data as d/δ becomes very small. At moderate values of d/δ (fig. 3b), the boundary irregularities begin to influence the flow outside the laminar film, the boundary then being no longer effectively smooth. With increasing values of d/δ , the turbulence induced by the wall roughness becomes greater, until finally the flow at the boundary

is fully turbulent (fig. 3c). Under such circumstances, the function $\varphi(\sqrt{\tau_o/\rho}\ d/\nu) = \varphi'(d/\delta)$ of equation 7 becomes constant, since the velocity distribution is no longer dependent upon viscosity. Thus, as will be seen from figure 2, for very large values of d/δ the experimental points approach the horizontal asymptote

$$\frac{v}{\sqrt{\tau_o/\rho}} - 5.75 \log \frac{y}{d} = 8.48 \qquad (9)$$

Because of the interdependence of velocity distribution and boundary resistance, it may also be shown (7) that

$$\frac{v}{\sqrt{\tau_o/\rho}} - 5.75 \log \frac{y}{d} = \frac{2.83}{\sqrt{f}} - 5.75 \log \frac{r_o}{d} + 3.75 \qquad (10)$$

the resistance factor for very smooth boundaries varying in the form

$$\frac{1}{\sqrt{f}} = -0.8 + 2 \log(R\sqrt{f}) \qquad (11)$$

while for fully effective boundary roughness,

$$\frac{1}{\sqrt{f}} = 1.74 + 2 \log \frac{r_o}{d} \qquad (12)$$

Figure 2 is thus seen to include two series of experimental data, one determined on the basis of velocity measurements, the other from measurements of resistance. The close agreement between the two series is good evidence of the validity of both relationships, the experimental points following a single functional trend between the limits of smooth and rough boundary flow.

Since the artificial roughness used in these experiments had essentially the same texture as that of a leveled sand bed in a laboratory flume, the foregoing relationships should be directly applicable to the study of the beginning of bed-load movement. This method of attack was adopted by Shields (12), who reasoned that the initial movement of material of any given particle size would require the existence of a certain critical velocity, v_c, at a distance above the bed proportional to the sediment diameter, $y_c = \alpha_1 d$. Thus, from equation 7,

$$v_c = \sqrt{\frac{\tau_o}{\rho}} \left[5.75 \log \alpha_1 + \varphi\left(\frac{d}{\delta}\right)\right] = \sqrt{\frac{\tau_o}{\rho}}\ \varphi_1\left(\alpha_1, \frac{d}{\delta}\right) \qquad (13)$$

The force exerted by the flow under these conditions is expressible in the form

$$F = \zeta d^2 \rho \frac{v_c^2}{2} \tag{14}$$

in which ζ is a coefficient of resistance to flow, depending in magnitude upon the sediment characteristics and a Reynolds number for local flow conditions; that is,

$$\zeta = \varphi_2\left(\alpha_2 , \frac{v_c d}{\nu}\right) \tag{15}$$

Introducing v_c from equation 13,

$$\zeta = \varphi_2\left[\alpha_2 , \sqrt{\frac{\tau_o}{\rho}} \frac{d}{\nu} \varphi_1\left(\alpha_1 , \frac{d}{\delta}\right)\right] = \varphi_3\left(\alpha_1 , \alpha_2 , \frac{d}{\delta}\right) \tag{16}$$

whence,

$$F = \varphi_3\left(\alpha_1 , \alpha_2 , \frac{d}{\delta}\right) d^2 \rho \frac{\tau_o}{2\rho}\left[\varphi_1\left(\alpha_1 , \frac{d}{\delta}\right)\right]^2 = \frac{\tau_o d^2}{2} \varphi_4\left(\alpha_1 , \alpha_2 , \frac{d}{\delta}\right) \tag{17}$$

The resistance to movement, on the other hand, will vary with the effective weight of the immersed sediment and with the form and arrangement of the grains:

$$R = \alpha_3\left(\gamma_s - \gamma\right) d^3 \tag{18}$$

At the beginning of motion, it is evident that R must equal F, whence,

$$\alpha_3\left(\gamma_s - \gamma\right) d^3 = \frac{\tau_c d^2}{2} \varphi_4\left(\alpha_1 , \alpha_2 , \frac{d}{\delta}\right) \tag{19}$$

in which T_c has its customary significance of critical tractive force, i. e., the intensity of boundary shear at the beginning of motion. Since α_1, α_2 and α_3 all depend upon the characteristics of the bed material, each should be expressible in terms of parameters representing, statistically, particle shape, grading, and compaction. Under such conditions, d properly refers to a geometric mean size of grain. On the other hand, if the materials to be studied are essentially uniform in size, shape, and compaction, equation 19 becomes simply

$$\frac{\tau_c}{\left(\gamma_s - \gamma\right) d} = \varphi\left(\frac{d}{\delta}\right) \tag{20}$$

Shields conducted a series of experiments on the initial movement of uniform materials having a wide range in specific weight, plotting results according to equation 20 as shown in figure 4. At once apparent is the great similarity of the functional trend to that of measurements on rough pipes in figure 2. In other words, the initial movement of bed particles is directly influenced by the conditions of motion in the neighborhood of the bed. The 45° line at the left, representing undisturbed laminar flow at the bed, has been fitted by eye, and follows the equation

$$\frac{\tau_c}{(\gamma_s - \gamma)d} = \frac{0.01}{d/\delta} \qquad (21)$$

Similarly, the horizontal line at the right representing fully developed turbulence at the bed is given by the equation

$$\frac{\tau_c}{(\gamma_s - \gamma)d} = 0.06 \qquad (22)$$

It is obvious that initial movement may occur within the laminar boundary layer, but that the influence of viscosity upon such movement steadily decreases as the boundary layer is broken up by grains of increasing relative size.

Of definite academic importance is this study by Shields, in that it shows for the first time the effect of viscous action on the beginning of movement. Its direct application is limited, however, to the choice of materials for model studies, since beds in natural streams display neither the initial regularity nor the grain uniformity of the laboratory study. Of perhaps even greater importance, therefore, is the fact that Shields found the form of initial bed irregularities to depend directly upon the magnitude of d/δ . At low values of this ratio, for instance, short, deep ripples developed. As the influence of viscosity decreased, the ripples tended to become shallower and longer, approaching a limit when the boundary layer was finally broken up completely. Evidently, the use of coarse, low-density materials such as pumice, amber, and lignite to simulate bed sediment in river models tends to decrease the influence of viscosity upon the bed development.

As T increased beyond the critical value T_c (following the direction of the arrows in fig. 4, since $T \sim 1/\delta^2$), the bed irregularities were found to increase in depth, but at the same time the rate of bed movement became greater. Shields reasoned that the sediment transport should be expressible in terms of discharge, slope, and the bed parameter $(\tau - \tau_c)/(\gamma_s - \gamma)d$,

once the motion at the bed became fully turbulent, namely, independent of the fluid viscosity. An analysis of measured data (fig. 5) proved that the transport function could be written in the dimensionless form

$$\frac{G}{Q} = 10\, S\, \frac{T - T_c}{(\gamma_s - \gamma)d} \qquad (23)$$

the factor G representing the rate of sediment transport by weight (measured under water), and Q the rate of water discharge, also by weight (this relationship may, of course, be written in a number of equivalent forms through introduction of the equilibrium equation for boundary shear, $T = \gamma D S$, and the Chezy equation, $V = C\sqrt{DS}$.) At low values of $(T-T_c)/(\gamma_s - \gamma)d$, the movement consisted of rolling or sliding along the bed, but at more advanced stages the sediment grains were carried over the bed irregularities in the process known as saltation. Movement finally became so pronounced that the crests of the irregularities were washed away--- at approximately $(T-T_c)/(\gamma_s - \gamma)d = 0.2$. Few experimental data are shown beyond this zone, for the turbulence of the flow, once saltation developed to a sufficient degree, would carry the saltating material into suspension (see fig. 4).

Equation 23 must be regarded as essentially empirical, in particular since it was based upon measurements with material having less than a two-fold variation in size, and restricted to conditions under which the material moved only as bed load. Nevertheless, were the relationship sufficiently well founded to warrant extrapolation, it could also be used to predict the total amount of material carried by the flow in more advanced stages of suspension. Although the actual function may not be linear even in the region shown in figure 5, there is no reason to expect an abrupt discontinuity at any point. Nevertheless, the possibilities of developing such a general relationship do not seem to have been investigated. Experimental measurements invariably cease once an appreciable amount of sediment goes into suspension, due, in part to the difficulty of trapping all material in the usual bed-load flume, and in part to the custom of regarding sediment suspension as a phenomenon of totally different category.

Turbulence and Suspended Load

Owing to the belief that flow conditions in the bed region differ from those at some distance above the bed, previous studies of the mechanics of suspension have, in turn, eliminated the bed zone from consideration. Thus limiting the analysis to regions of

fully developed turbulence, it has repeatedly been shown that the sediment concentration at any level (fig. 6) should vary according to the function

$$\varepsilon \frac{dc}{dy} = -cw \qquad (24)$$

Herein c represents the concentration of the suspension in percent by weight, w is the terminal velocity of settling of the sediment grains in stagnant water, and ε is a kinematic turbulence coefficient, corresponding roughly to the kinematic viscosity--that is, while ν is a measure of the intensity of molecular mixing, ε refers to a molar mixing process in which finite masses of fluid participate in eddy motion. This process of intermixing between neighboring regions of flow tends to make the sediment distribution more uniform by carrying material in the direction of decreasing concentration--upwards, in the normal case--at a rate proportional to the intensity of mixing and to the rate of change of concentration at that level. Because of the weight of the sediment, on the other hand, material tends to move downwards at a rate proportional to the concentration at that level and to the velocity of settling. The state of equilibrium described by equation 24 presumes the effects of settling and mixing to be in balance for all values of y at which the flow is turbulent.

Since the mixing coefficient is dimensionally equivalent to the product of a velocity and a length, the velocity may be considered proportional to v'_y, the mean absolute velocity of the eddy currents in the vertical direction, and the length, ℓ, proportional to either the average size of the eddies or the vertical distance the fluid masses are carried before losing their identity in the surrounding fluid. While the fall velocity, w, refers to a specific size of sediment, ε must be regarded purely as a statistical mean product, both v'_y and ℓ varying with time in accord with the normal error law. It is pointless, therefore, to presume that w must be smaller than the mean absolute value of v'_y before suspension may exist, for there is no limit to the magnitude of instantaneous fluctuations. However, equation 24 does require that the mixing of the sediment carried by the eddies be statistically the same as, or at least proportional to, that of the fluid itself. The mixing coefficient should thus be written as

$$\varepsilon = \beta v'_y \ell \qquad (25)$$

in which β is a bulk coefficient of proportionality.

The general validity of equation 24 was verified within the past year by means of an agitating mechanism producing a constant intensity of mixing throughout a tank of water (11). Under such circumstances $\mathcal{E}$ becomes independent of y, whereupon equation 24 may be integrated to yield the concentration at any level in its ratio to that at some arbitrary level a (see fig. 6); thus

$$\frac{c}{c_a} = e^{-\frac{w(y-a)}{\mathcal{E}}} \qquad (26)$$

Four different sizes of uniform quartz sand were tested, permitting an approximately 30-fold variation in fall velocity. The magnitude of $\mathcal{E}$ varied directly with the frequency of agitation, which could be controlled mechanically over an 8-fold range. Curves of sediment distribution could be determined from pipette samples taken over a vertical distance of 1 1/2 feet. Not only were the various sizes investigated individually, but a mixture of all four grades was tested at various values of $\mathcal{E}$, yielding the composite dimensionless plot shown in figure 7. Aside from secondary deviations (due to variations in both β and w for the coarse material in the presence of fine), the points follow the exponential curve of equation 26 in a satisfactory manner.

Application of equation 24 to the suspension of sediment in flowing water is a more difficult matter, since $\mathcal{E}$ then varies as a function of y. For want of knowledge as to its actual variation in an open channel, one is compelled to turn again to studies of flow in pipes. In deriving expressions for velocity distribution and resistance (refer to fig. 8), Prandtl assumed that the mean absolute component of fluctuation in the direction of flow, v'_y, would be proportional to the product of the mixing length and the mean velocity gradient ($v'_x \sim \ell\, dv/dy$), and that the components of fluctuation in the two directions would be proportional to each other ($v'_x \sim v'_y$). Since, as shown by Reynolds, the intensity of shear varies with the mean product of the fluctuations ($\tau = -\rho \cdot \overline{v'_x v'_y}$), and since intensity of shear is distributed linearly along the pipe radius according to the expression $\tau = \tau_o\,(1 - y/r_o)$, it will be seen that the following equations for v'_y, ℓ, and $\mathcal{E}$ (assuming ℓ and v'_y to absorb the proportionality factors) should then hold:

$$v'_y = \sqrt{\frac{\tau}{\rho}} = \sqrt{\frac{\tau_o}{\rho}\left(1 - \frac{y}{r_o}\right)} \qquad (27)$$

$$\ell = \frac{\sqrt{\tau/\rho}}{dv/dy} = \sqrt{\frac{\tau_o}{\rho}}\,\frac{\sqrt{1-y/r_o}}{dv/dy} \qquad (28)$$

$$\varepsilon = \frac{\tau/\rho}{dv/dy} = \frac{\tau_o}{\rho}\,\frac{1-y/r_o}{dv/dy} \qquad (29)$$

The variation of v'_y appears to be independent of the velocity gradient, and is plotted in dimensionless form as curve A of figure 9. This curve is seen to extend from zero at the axis to a maximum at the wall. However, Prandtl did not intend equations 27, 28, and 29 to apply at either of these points, for v'_x and v'_y are not necessarily proportional in those zones, and dv/dy is equal to zero at the axis. Actual measurements of v'_y (in air with a hot-wire anemometer) (13) yield curve B of figure 9, which is seen to have a finite value at the axis, to increase toward the wall, and finally to drop off abruptly. The effect of the unknown proportionality factor is indicated by the displacement of the two curves.

Nikuradse determined the trends of ℓ and ε from the slope of measured velocity-distribution curves in both smooth and rough pipes, as shown by curves C and G in figures 10 and 11. The magnitude of ℓ was assumed to attain a maximum value at the axis, where one would expect the eddies to have the greatest size, although equation 28 actually becomes indeterminate when $y/r_o = 1$ and $dv/dy = 0$. The magnitude of ε in equation 29 becomes indeterminate for the same reason, although ε will approach zero if v'_y does.

While equations 3 and 9 were developed for the velocity distribution in the wall region, they have been found to agree with measurements almost as far as the pipe axis. Differentiation of either expression would indicate that dv/dy is inversely proportional to y, which yields curves D and H of figures 10 and 11. Both ℓ and ε now reach zero at the axis as well as at the wall. On the other hand, Von Kármán's similarity hypothesis for turbulence in the intermediate zone between wall and axis led to the expression $\ell = \kappa\,(dv/dy)/(d^2v/dy^2)$, introduction of which into equations 28 and 29 results in curves E and I for ℓ and ε. Curve F was derived in a statistical treatment of turbulence by Gebelein (2).

Despite the departure of these several curves from one another in both form and position, the corresponding expressions for velocity distribution and resistance are in sufficient agreement with measurements for all practical purposes--even when applied to uniform flow in open channels (except for possible adjustment of constants). On the other hand, since the distribution of suspended matter depends directly upon $\mathcal{E}$ as a function of y, one hesitates to use any of these distribution curves without further experimental check. Unfortunately, the hot-wire method of measuring turbulence in air does not seem to be suited to use in water; and the simulation of a water surface with air as the model fluid is obviously out of the question. Several alternative methods are now in an early state of development (4, 8, 3), but as yet no usable open-channel measurements are at hand.

Leighly (5), Christiansen (1), and others have sought to correlate the distribution of sediment and velocity in actual streams by determining dv/dy from measured velocity profiles and then computing $\mathcal{E}$ from equation 29. Such results, however, are no more dependable than Nikuradse's curve G, for the reasons already stated. Moreover, there is not yet sufficient evidence to show whether the magnitude of $\mathcal{E}$ determined from equation 29 is numerically equal, or merely proportional, to that for the sediment suspension even in the zone for which this equation indicates the proper functional trend.

Whatever the true analytic relationship between $\mathcal{E}$ and y, certain general conclusions may be drawn by adopting one which does not depart too seriously from probable conditions. The frequent assumption that $\mathcal{E}$ is constant over the entire flow section is, of course, far from the truth, although it may become more nearly constant some distance from the boundary than is indicated by the curves of figure 11. At a free surface both $\mathcal{E}$ and v'_y are undoubtedly smaller than at the axis of a pipe, approaching zero if the free surface is smooth; that $\mathcal{E}$ does not always approach zero as a limit is indicated by visible disturbances at the surface of a very turbulent stream.

Thus, except very close to the bed and to the surface, either curve H or curve I may still indicate the general trend of $\mathcal{E}$ in a wide channel. Selecting H as the simpler of the two, equation 24 may be integrated to yield

$$\frac{c}{c_a} = \left(\frac{D/y - 1}{D/a - 1}\right)^z \qquad (30)$$

wherein $z = w/\kappa\sqrt{\tau/\rho} = w/\kappa V\sqrt{f/8}$. In a semi-logarithmic diagram, the relative position of the distribution curve should then be governed by the magnitude of z , and the form by the magnitude of D/a ; the parameter a need be only so great as to insure fully developed turbulence for all positive values of y . Figure 12 thus shows schematically a series of relative distribution curves for multiple values of z and for $D/a - 1 = 10$.

As has already been remarked, any relationship of this form will not yield absolute values of sediment concentration, for it provides no means of evaluating c_a . On the other hand, once the concentration and settling velocity of each grain size at level a are known, the absolute distribution curves for each size may be obtained. Thus, from a sample of the suspension at the reference level, one could determine the settling velocities and the absolute curves for each value of w included in the sample, integrate the product cv for each curve, and then add all together to obtain the total rate of transport of suspended load above the reference level. This procedure would obviously be a tedious one, and would have to be repeated for every change of flow conditions. One is therefore inclined to seek a more convenient relationship in terms of average sediment parameters.

As in the case of the distribution of particle size, an analysis of the fall-velocity characteristics of a sediment sample may be plotted in histogram form (fig. 13a), the abscissa scale representing the logarithm of w and the ordinate scale the concentration c per class interval. The resulting block diagram will approach a smooth weight-frequency diagram as the class interval becomes small, the area enclosed by this curve being equal to the concentration C of the total material in the sample. If one assumes curve A to represent the weight-frequency distribution of w at the reference level a , it will be found that the frequency curves at various levels above a will be as shown in figure 13b for the function $\varepsilon = \varphi(y/D)$ plotted in figure 12--the enclosed areas again representing the magnitudes of C at the respective levels.

Were c and C identical at every level (that is, were the entire range of w only one class interval), it is evident that the vertical distribution curves for C would coincide in figure 12 with the corresponding curve for $z = w/\kappa\sqrt{\tau/\rho}$. For a given value of $\kappa\sqrt{\tau/\rho}$, actual departures from this limiting case will depend primarily upon the geometric mean abscissa w_m of the

w-frequency curve at the level a , secondarily upon the extent to which w deviates from this mean, and to a practically negligible degree upon the skewness or asymmetry of the curve. For instance, curves A, B, and C of figure 13 display the same proportional variation of w , but differ in geometric mean; for such frequency curves at level a , the departure of the respective distribution curves for C/C_a from those of c/c_a for the corresponding values of w_m will be seen from figure 12, the difference evidently increasing with increasing values of $w_m/\kappa\sqrt{\tau/\rho}$. Similarly, curves B and D , or C and F , have, respectively, the same means but different deviations from these means; the departure is seen to decrease with decreasing values of $w_m/\kappa\sqrt{\tau/\rho}$ and of the deviation. On the other hand, the extreme skewness of the frequency diagrams F and G is seen to have little effect upon the distribution of C/C_a , the corresponding distribution curves in figure 12 varying to a relatively small extent from that for the symmetrical diagram C having the same mean and deviation.

The magnitudes of the geometric mean and the standard deviation of a frequency curve may be shown statistically to correspond to the abscissa of the center of gravity of the enclosed area and to the radius of gyration of the area about a vertical axis through this point. These parameters may be taken directly from a cumulative plot of the frequency curves of logarithmic probability paper. On such a plot of frequency diagram, having the symmetrical form of normal error curve, will become a straight line, varying in position with the geometric mean and in slope with the standard deviation. The value of w_m will correspond to the intersection of the cumulative line with the 50 percent ordinate, while σ_w , the standard geometric deviation (i. e., antilogarithm of the standard deviation), may be found by dividing the 84.1 percent intercept by w_m or w_m by the 15.9 percent intercept. For example, from figure 14 it is seen that curves B and D , A , and C and E yield values of w_m equal respectively to $1/8, \sqrt{2}/4,$ and 1 cm/sec.; likewise, for A , B , and C, $\sigma_w = 2$, while for D and E , $\sigma_w = \sqrt{2}$. In the case of skewed curves, a close approximation may be made through use of two terms of a logarithmic Gram-Charlier series, which yields a family of curves coinciding at the 84.1 percent and 15.9 percent intercepts with a straight line having the same geometric mean and standard deviation. As seen from curves F and G in figure 14, the corresponding values of w_m and σ_w may be read on the straight line passing through these intercepts.

From the foregoing discussion of the various parameters governing the distribution of suspended load, it follows that the

distribution of C/C_a over the vertical section will depend upon the three dimensionless parameters a/D, $w_m\sqrt{\tau/\rho}$, and σ_w, for a given distribution of ε. Since the distributions of both ε and v are governed only by the mean velocity and the relative roughness of the bed in fully turbulent flow, it would appear that the total transport of suspended load might eventually be expressed in terms of a few pertinent parameters characteristic of the boundary, of the flow, and of the sediment--a method of approach which will be discussed further in the following section on Prediction of Total Load.

Before leaving the subject of sediment characteristics, several points will bear elaboration. Despite the significance of the fall velocity in the study of suspended load, it is general practice to determine the size-frequency, rather than the w-frequency, characteristics of sediment samples. Sieving is used, so far as possible, with recourse to the pipette or other hydraulic methods for material passing the 200-mesh sieve. It so happens that sediments finer than 200 mesh will generally settle in water in close accordance with Stokes' law, $w \sim d^2$; while the settling of coarser materials will approach the limit $w \sim d^{\frac{1}{2}}$ as d becomes increasingly greater (10). Moreover, sieve analysis does not indicate true hydraulic diameter (that of a sphere having the same density and settling velocity), since it does not properly evaluate shape and density factors. Prediction of the w-frequency from the size-frequency curve is therefore at best uncertain; and because w-frequency and size-frequency curves lying in part beyond the Stokes' range will have different degrees of skewness, it cannot be expected that w_m and σ_w will always correspond to the geometric mean and the standard geometric deviation of the size-frequency diagram. A direct method of determining the w-frequency of coarse material as well as fine has still to be perfected.

In this regard, it should be noted that material finer than about 15 microns will almost invariably flocculate, except in streams in arid climates. Obviously, laboratory analysis of deflocculated samples may yield grading curves which bear no relation to the w-frequency of the actual suspension. This danger could be obviated by analysis of suspended matter in the stream water obtained with the sample. It might be added that in suspensions of appreciable concentration the settling velocity of coarse particles in the presence of fines is less than in clear water. The question remains for the present an academic one, for the analysis of turbulence has not yet advanced to the treatment of density variation across the flow section.

Prediction of Total Load

Mention was made at the end of the section on Turbulence and Bed Load of the fact that the transport function for bed load alone might well be extended empirically beyond the zone of appreciable saltation and thus used to predict the total load of a stream. In the same manner, one is inclined to speculate on the possibility of estimating the total stream load through use of only the function for suspended load. The latter is by far the more venturesome method of attack, but it would seem at the present time to provide the sole analytical means of expressing the transport capacity of a stream in terms of readily measurable bed and flow parameters.

Since such a method would evidently require extrapolation of the suspended-load function well into the bed region, it would first be well to note the reason why this procedure has hitherto been avoided. If the reference level in equation 30 is placed at the bed itself, a becomes equal to zero, and inspection of the equation will show that the concentration will also be zero over the entire section. In other words, the fact that ε in equation 29 becomes zero at the wall would indicate, paradoxically enough, that no sediment can be lifted off the bed, although an indefinite amount may be held in suspension once it rises above the level of zero mixing.

"Held in suspension" is a phrase which has a purely statistical significance, for the process of turbulent mixing entails a continuous interchange of material between neighboring levels of the flow. The presence of material in suspension therefore indicates not only that it was originally lifted from the bed in one way or another, but that some means continues to exist whereby new material may be carried into suspension to replace that constantly settling out. In other words, either ε does not reach a value of zero at the bed, or else the momentary fluctuations from a statistical mean value of zero are sufficient to provide the initial upward impulse.

With reference to figure 3c, it is apparent that in the absence of viscous influence the bed roughness may be considered to produce local disturbances depending in size upon the parameter k and in intensity upon the mean velocity at the distance k from the mean bed level. While these eddies may actually yield a zero magnitude of ε at zero elevation if evaluated in a statistical sense, the local effectiveness of the mixing process surely extends even below the mean level of the bed. It does not seem unreasonable, therefore, to presume that ε remains essentially constant from $y = k$ to $y = 0$.

Under these circumstances, k would serve as the limiting value of a in equation 30. The magnitude of C_k might then be approximated from equation 26, using for the constant magnitude of ε that at $y = k$, and for C_o the concentration of the bed material. It is barely possible, moreover, that a might be set equal to some constant fraction of k, C_a then being taken equal to C_o and the intermediate step using equation 26 being omitted completely.

The latter assumption is obviously a bold one. In fact, either procedure must be subjected to thorough experimental check before it can be considered valid. Experimental measurements would be necessary in any case, moreover, to determine the proper numerical value of k. Nikuradse, it will be recalled, adopted the grain diameter as a measure of roughness, although the effective height of the irregularities in the sand coating that was applied to the pipe was not necessarily the same as the diameter of the grains themselves. Shields also used the grain diameter as a measure of roughness in the case of initial movement; as bed undulations develop in size, however, the individual sediment grains no longer determine the absolute bed roughness, k then varying with the size and shape of the undulations.

Equation 12, with possible modification of constants, might still be used to estimate the effective magnitude of k for an open channel, for this relationship has both analytical and experimental foundation. Engineers, on the other hand, are more accustomed to thinking in terms of the Chezy equation

$$V = C\sqrt{RS} \tag{31}$$

in which C is inversely proportional to the square root of the resistance coefficient, f:

$$C = \sqrt{\frac{8g}{f}} \tag{32}$$

C may therefore be evaluated either in terms of the relative roughness of equation 12, or, as is more customary, through use of the empirical formula of Manning:

$$C = \frac{1.486\, R^{\frac{1}{6}}}{n} \tag{33}$$

Although it is not generally realized, the Manning n is the sixth root of an absolute roughness parameter, n^6/R representing a

relative roughness similar to the d/r_o used by Nikuradse. The Manning relationship therefore applies to flow in which the influence of viscosity is negligible. If equation 33 were truly valid, n^6 would be directly proportional to values of $k = d$ determined from equation 12. The actual relationship may be seen from figure 15, which may be used to estimate at least the order of the magnitude of the absolute roughness from measurable flow parameters.

Whether or not the foregoing means of predicting total load proves feasible, the method of analysis suggests a systematic organization of the variables belonging in a general transport function. It was shown in the section on Turbulence and Suspended Load that the distribution curve for suspended load is a function of the material characteristics at the reference level, the height of the reference level in its ratio to total depth, the friction velocity, and the distribution of $\mathcal{E}$. Setting a equal to k, these parameters may be grouped dimensionlessly in the functional form

$$\text{Quantity in suspension} = \varphi_1\left(C_K, \frac{k}{D}, \frac{\sqrt{T/\rho}}{w_m}, \sigma_w\right) \qquad (34)$$

the suspension increasing with the magnitude of each dimensionless term. The form of the function depends, evidently, upon the distribution of $\mathcal{E}$; but, once established, the variation of $\mathcal{E}/D\sqrt{T/\rho}$ should remain a unique function of y/D alone.

The magnitude of C_k, in turn, should vary with the bed concentration, the absolute roughness, the mean fall velocity and its standard geometric deviation, and the effective mixing at the bed, that is,

$$C_K = \varphi_2\left(C_o, \frac{\mathcal{E}_K}{K w_m}, \sigma_w\right) \qquad (35)$$

If $\mathcal{E}_K$ is evaluated in terms of k and v_k, v_k being found from equation 9, it will then be seen that

$$C_K = \varphi_2'\left(C_o, \frac{\sqrt{T/\rho}}{w_m}, \sigma_w\right) \qquad (36)$$

If this value of C_k is used in equation 34, the form of the function will change, but except for C_o the parameters will be the same as before.

For fully effective boundary roughness it has been shown that the velocity distribution is a function of the friction

velocity and the relative roughness, both parameters already appearing in the foregoing relationships. It should therefore be possible to express the total material transported in the form

$$\frac{G_s}{Q} = \varphi_3\left(C_o, \frac{k}{D}, \frac{\sqrt{\tau/\rho}}{w_m}, \sigma_w\right) \qquad (37)$$

This expression for total load, evidently, is the counterpart of the empirical bed-load equation, likewise requiring experimental determination of the functional form and the magnitude of the numerical constants. However, the resulting relationship will not be entirely empirical because of the choice and arrangement of the variables by analytical means. If it is truly general, on the other hand, it should describe the earlier stages of movement at least as well as does the bed-load function. As a matter of fact, when simplified to the form

$$\frac{G_s}{Q} \sim \frac{k\sqrt{\tau/\rho}}{D\, w_m} \qquad (38)$$

it will be found to be essentially the same as the Shields expression (equation 20), since $D \sim 1/S$, and $w/k \sim (\gamma_s - \gamma)d$ within the limited range of size which Shields studied.

Like the bed-load equation, the general relationship can be rewritten in other forms through introduction of the Chezy expression and the equilibrium equation for boundary shear, $\tau = \gamma DS$. In particular it should be noted that $\sqrt{\tau/\rho} = V\sqrt{f/8}$, while f in turn is a function of k/D; thus the friction velocity, $\sqrt{\tau/\rho}$, may be replaced by the mean velocity of flow, V, elimination of f merely changing the form of the general function. Equation 37 might then be written in the form

$$\frac{G_s}{Q} = \varphi\left(C_o, \frac{k}{D}, \frac{V}{w_m}, \sigma_w\right) \qquad (39)$$

Although this general function for total load may be valid even for relatively high sediment concentration, it must be noted that under such conditions the boundary roughness may not be fully effective. That is, the mechanical friction resulting from contact of the sediment grains in the zone of high concentration near the bed will tend to reduce the turbulence of the boundary flow--producing in the extreme case a region of non-turbulent movement at the bed roughly equivalent to the laminar boundary layer--mechanical friction now taking the place of fluid viscosity. This

circumstance, coupled with the failure of existing equations for velocity and sediment distribution to take into account an appreciable density gradient, makes the problem of high sediment concentration decidedly more complex than the conditions herein assumed.

Conclusion

Analysis of sediment transportation in the light of fluid turbulence at once emphasizes the need for experimental data, both to provide the necessary numerical constants for proved functional relationships and to test the validity of still unproved assumptions. One reason for the lack of such data has lain in the difficulty of systematizing research without some immediate experimental goal. It is to this end that the present analysis has been prepared, for it provides a definite program of research in the proof or disproof of methods herein proposed. By way of summary, therefore, it would seem expedient to outline the points in this analysis still awaiting experimental study, with suggestions as to suitable procedure.

(1) Shields' treatment of initial movement and subsequent transportation of material of uniform size and shape merits early investigation as to the effect of change in size and grading. Logical parameters for the arbitrary control of size distribution are the geometric mean diameter and the standard geometric deviation of size-frequency curves. Shape is probably of secondary importance in natural bed material.

(2) The problem of open-channel flow is replete with unknown factors, even for channels of very wide cross section. The logarithmic velocity-distribution and resistance relationships must be checked systematically, and numerical constants determined for cases of actual as well as artificial roughness. The distribution of v'_y , ℓ , and particularly ε must be determined--with apparatus still to be perfected.

(3) Even prior to the direct measurement of ε as a function of y , the distribution of suspended load may be correlated with the velocity distribution through controlled laboratory tests. It would be most expedient to avoid the dependence of the suspension upon bed-sediment roughness by securing artificial roughness elements (metal projections) to the flume bottom in such a manner that the bed material could circulate freely without altering the magnitude of the relative roughness. While this investigation might best begin with low concentrations of uniform material, the nature of the artificial roughness is such as to permit studies of the effects of grading and of high concentration upon the suspension in the simplest manner possible.

(4) Determination of stream capacity may proceed in two ways: First, the relationship may be sought between the suspended load and conditions at the bed, by investigating the possibility of evaluating the sediment-distribution function in terms of the bed roughness and the concentration of the bed material. Secondly, and of greater practical importance, a general function of the usual bed-load type may be extended to include total load by continuing experiments beyond the stage of appreciable saltation; evidently, the usual bed-load trap will not catch material in suspension, a vertical sampler of the divisor type being a possible substitute; whatever the experimental technique, the investigation must determine the functional relationship of dimensionless parameters similar to those in equation 39.

Tabulation of Symbols

a = reference level for suspended-load function.

c = sediment concentration by weight for given fall velocity.

d = diameter of sediment grains.

e = base of natural logarithms.

f = coefficient of resistance to flow.

g = acceleration of gravity.

k = absolute roughness of boundary.

l = length scale of turbulent mixing.

n = Manning roughness coefficient.

r_o = pipe radius.

v = mean velocity of flow at any point.

v'_x = velocity of fluctuation in direction of flow.

v'_y = velocity of fluctuation normal to boundary.

w = settling velocity of sediment.

w_m = geometric mean settling velocity.

y = normal distance from boundary.

z = exponent in the suspended-load function.

C = total concentration by weight at any level (also used locally for Chezy coefficient).

D = total depth of flow.

F = force exerted by flow on bed material.

G = rate of sediment discharge by weight.

Q = rate of total discharge by weight.

R = hydraulic radius (also used locally for resistance of bed material to initial movement).

$\mathfrak{R}$ = Reynolds number.

S = slope.

T = tractive force (intensity of shear at boundary).

T_c = tractive force at beginning of bed movement.

V = mean velocity of flow for cross section.

α = coefficient for sediment characteristics.

β = proportionality factor for mixing process.

γ = specific weight of fluid.

γ_s = specific weight of sediment.

δ = thickness of boundary layer.

ϵ = coefficient of turbulent mixing.

ζ = coefficient of sediment resistance to flow.

κ = flow constant, equal to about 0.40.

μ = dynamic viscosity.

ν = kinematic viscosity.

ρ = mass density.

σ_w = standard geometric deviation of w-frequency.

τ = intensity of fluid shear.

τ_o = intensity of shear at boundary.

φ = function of.

Literature Cited

(1) Christiansen, J. E.
Distribution of Silt in Open Channels. Amer. Geophys. Union Trans. Ann. Meeting 16 (pt. 2): 478-485. 1935.

(2) Gebelein, H.
Turbulenz. p. 114. Julius Springer, Berlin. 1935.

(3) Hubbard, C. W.
Investigation of Errors of Pitot Tubes. Amer. Soc. Mech. Engin. Trans. 1939.

(4) Kalinske, A. A., and Van Driest, E. R.
Applications of the Statistical Theory of Turbulence to Hydraulic Problems. 5th Internatl. Cong. Applied Mech. Proc.: pp. 416-421. Cambridge, 1939.

(5) Leighly, John
Toward a Theory of the Morphologic Significance of Turbulence in the Flow of Water in Streams. Univ. Calif. Press Publ. in Geog., v. 6, No. 1: pp. 1-22. 1932.

(6) Nikuradse, J.
Gesetzmässigkeiten der Turbulenten Strömung in Glatten Rohren. VDI Forschungsheft 356. 1932.
Strömungsgesetze in Rauhen Rohren. VDI Forschungsheft 361. 1933.

(7) Prandtl, L.
Aerodynamic Theory. v. 3: pp. 143-145. Julius Springer, Berlin. 1935.

(8) Richardson, E. G.
An Experimental Study of Turbulence Diffusion. Phys. Soc. Proc., v. 49. 1937.

(9) Rouse, Hunter
Modern Conceptions of the Mechanics of Fluid Turbulence. Amer. Soc. Mech. Engin., Trans. v. 102: pp. 463-554. 1937.

(10) ———
Nomogram for the Settling Velocity of Spheres. Ann. Rpt., Com. on Sedimentation, Natl. Res. Council. 1937.

(11) Rouse, Hunter
Experiments on the Mechanics of Sediment Suspension. 5th Internatl. Cong. Applied Mech. Proc., pp. 550-554. Cambridge, 1939.

(12) Shields, A.
Anwendung der Aehnlichkeitsmechanik und der Turbulenzforschung auf die Geschiebebewegung. Mitteilungen der Preussischen Versuchsanstalt für Wasserbau und Schiffbau, Heft 26, Berlin 1936. (Translations of this paper are on file with the Engineering Societies Library, the National Hydraulic Laboratory, and the U. S. Waterways Experiment Station.)

(13) Wattendorf, F. L.
Investigations of Velocity Fluctuations in a Turbulent Flow. Jour. Aeronaut. Sci. v. 3: pp. 200-202. 1936.

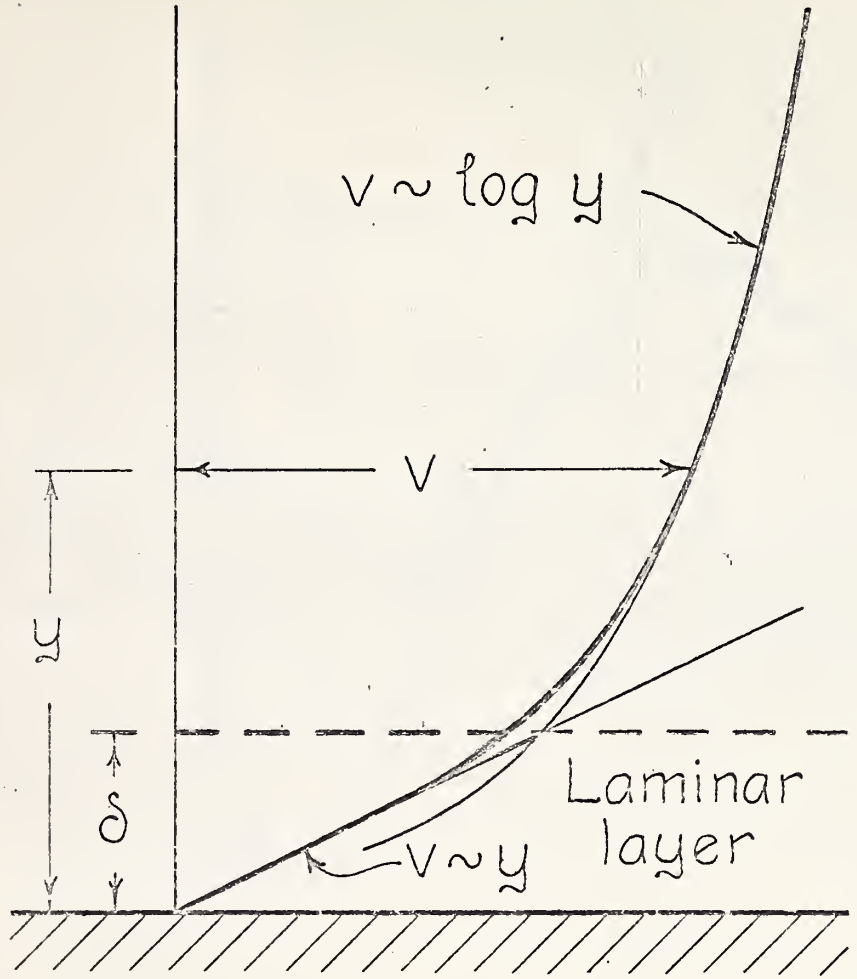

Fig. 1.
Velocity distribution near
a smooth boundary.

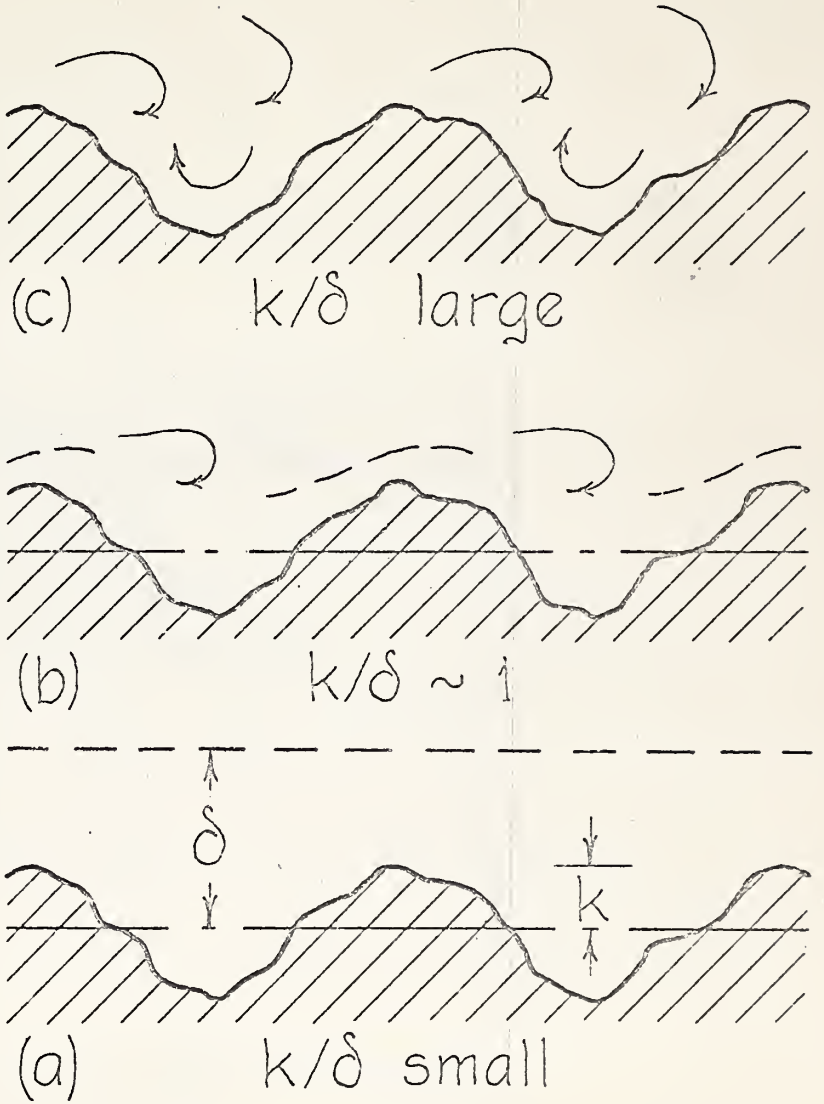

Fig. 3.
Development of turbulence
at a rough boundary.

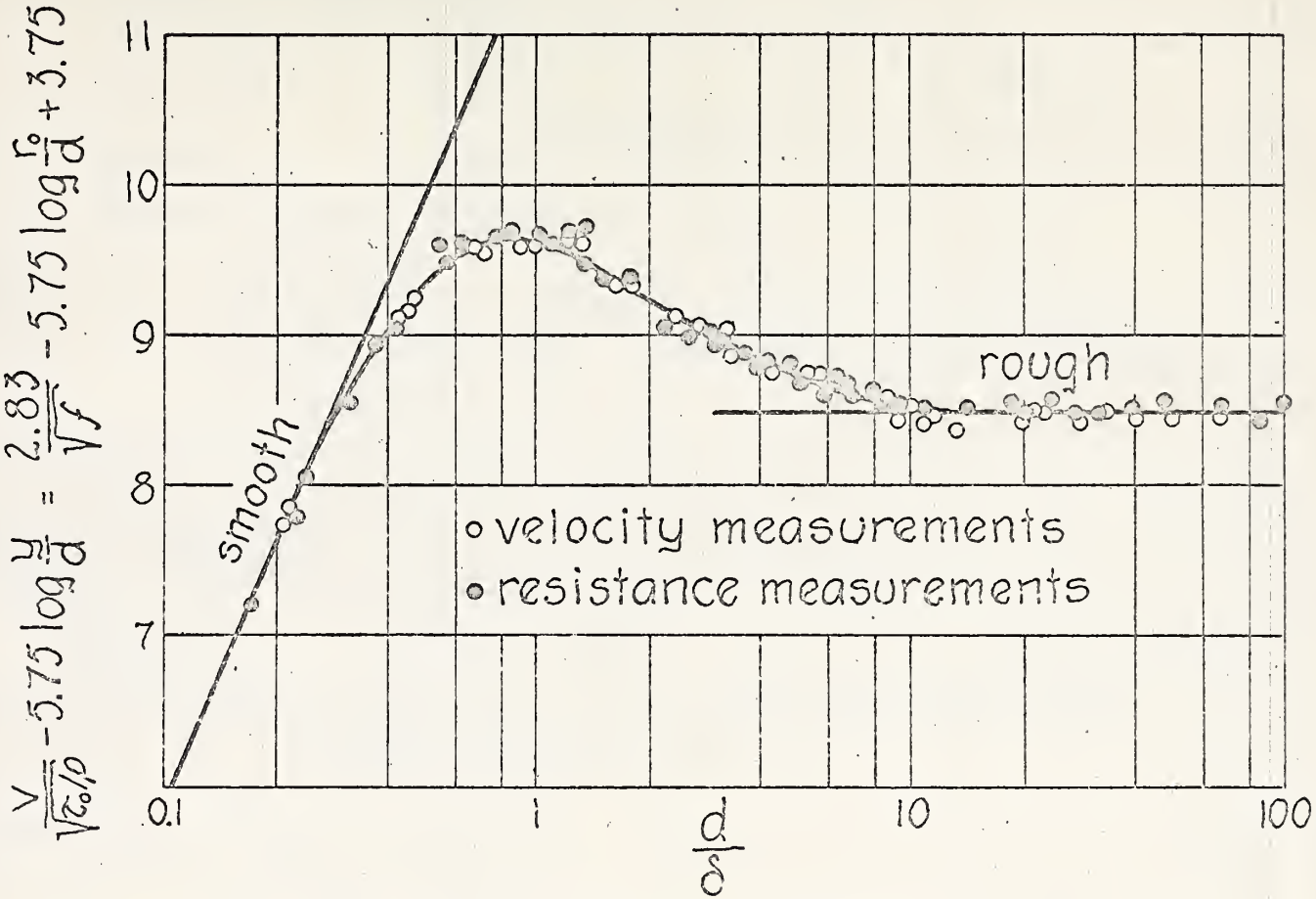

Fig. 2.

Influence of boundary-layer thickness upon velocity distribution and resistance for rough boundaries.

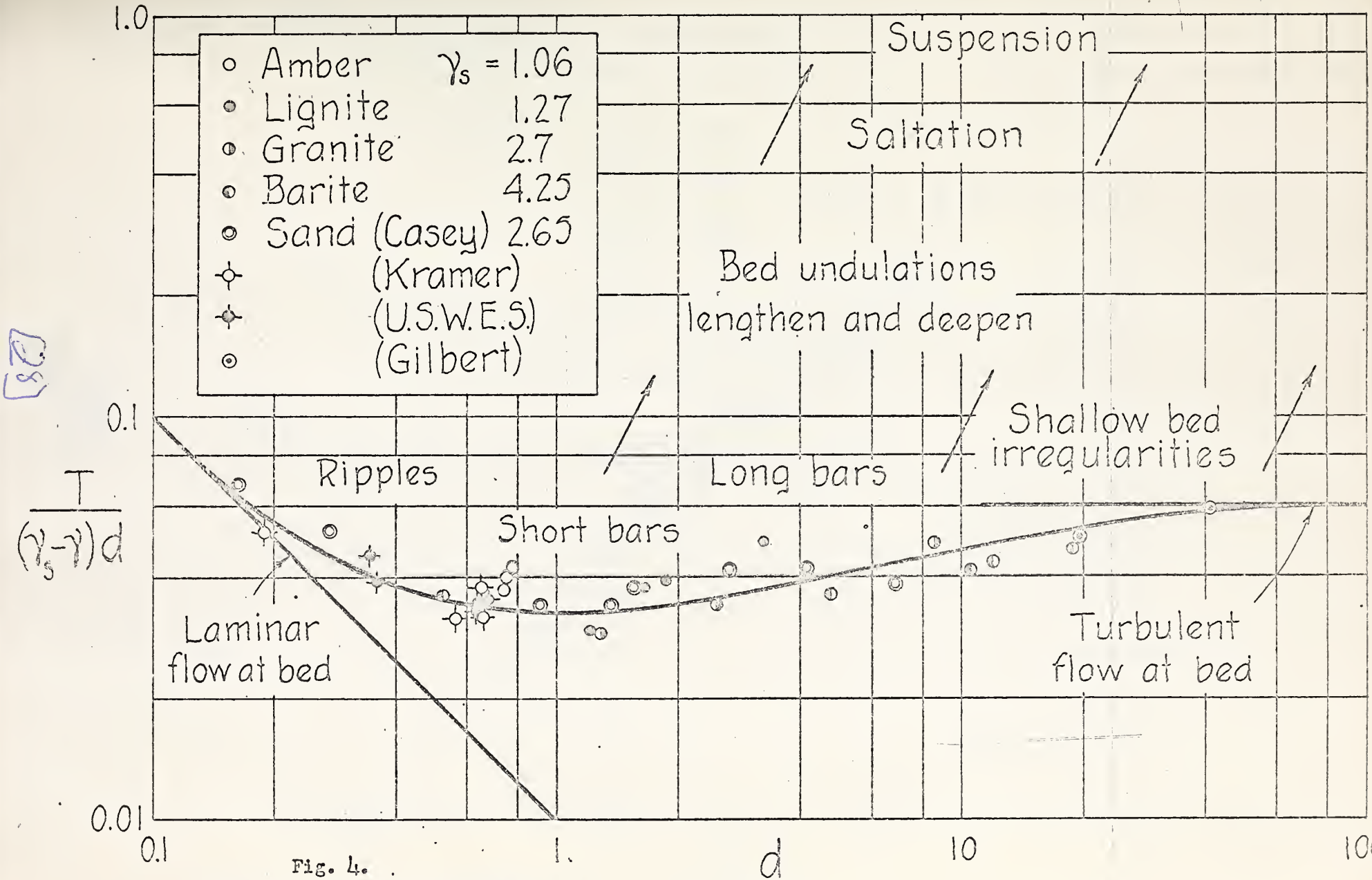

Fig. 4.

Beginning of bed-load movement as a function of grain diameter and boundary-layer thickness.

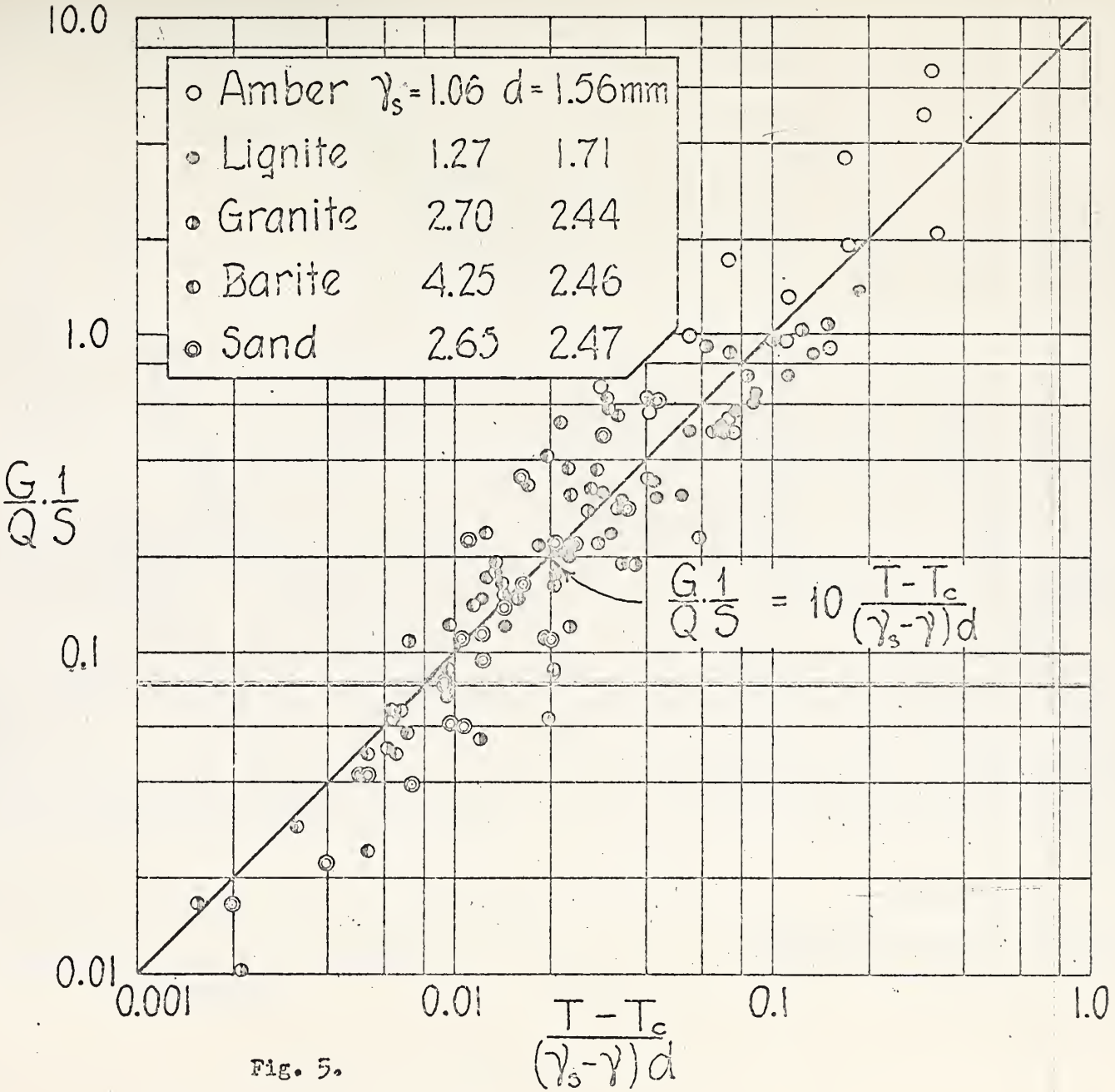

Fig. 5.
Transportation of bed-load.

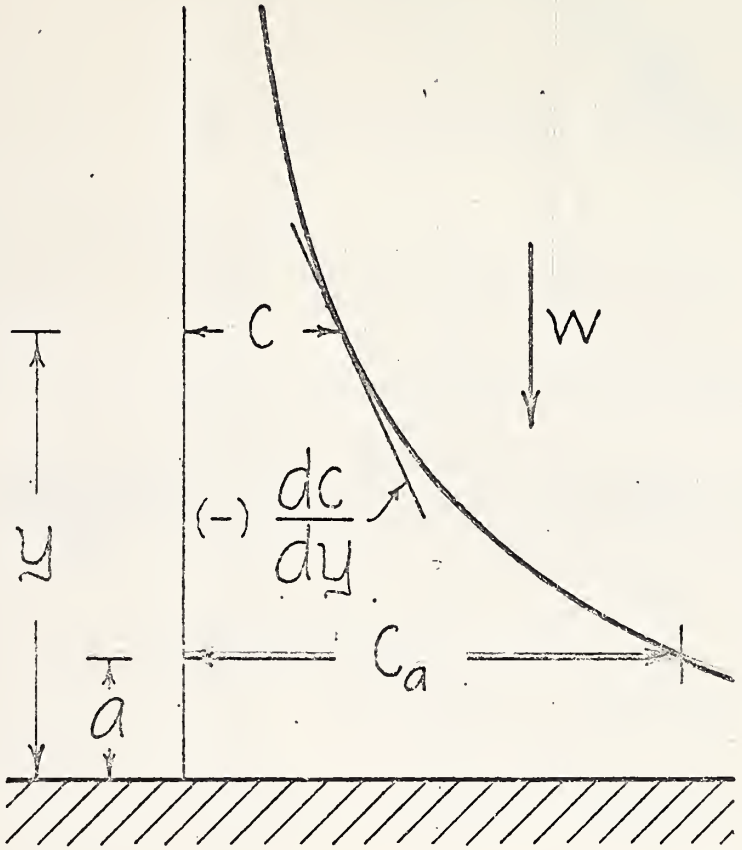

Fig. 6.

Definition sketch for sediment suspension.

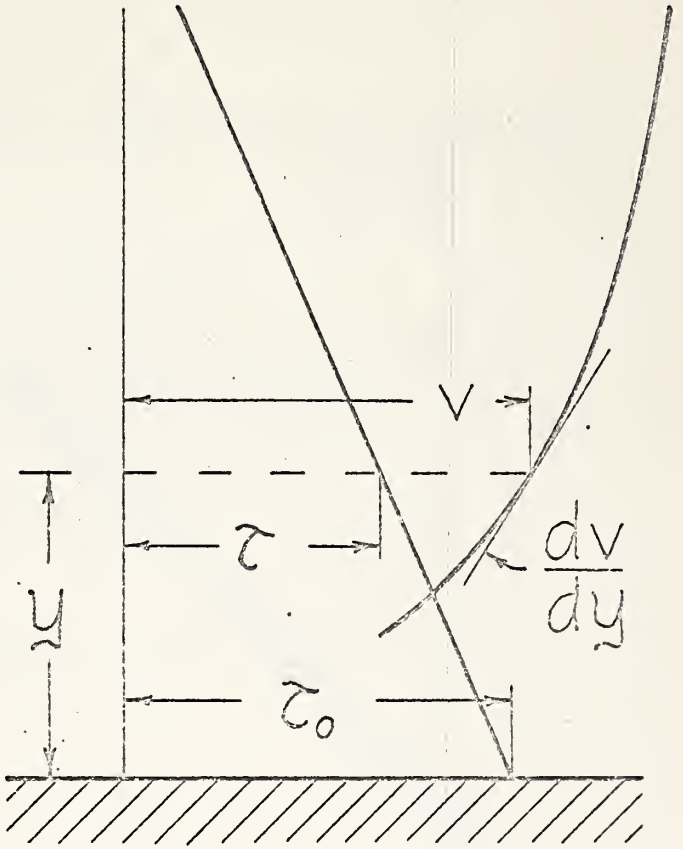

Fig. 8.

Definition sketch for velocity and shear.

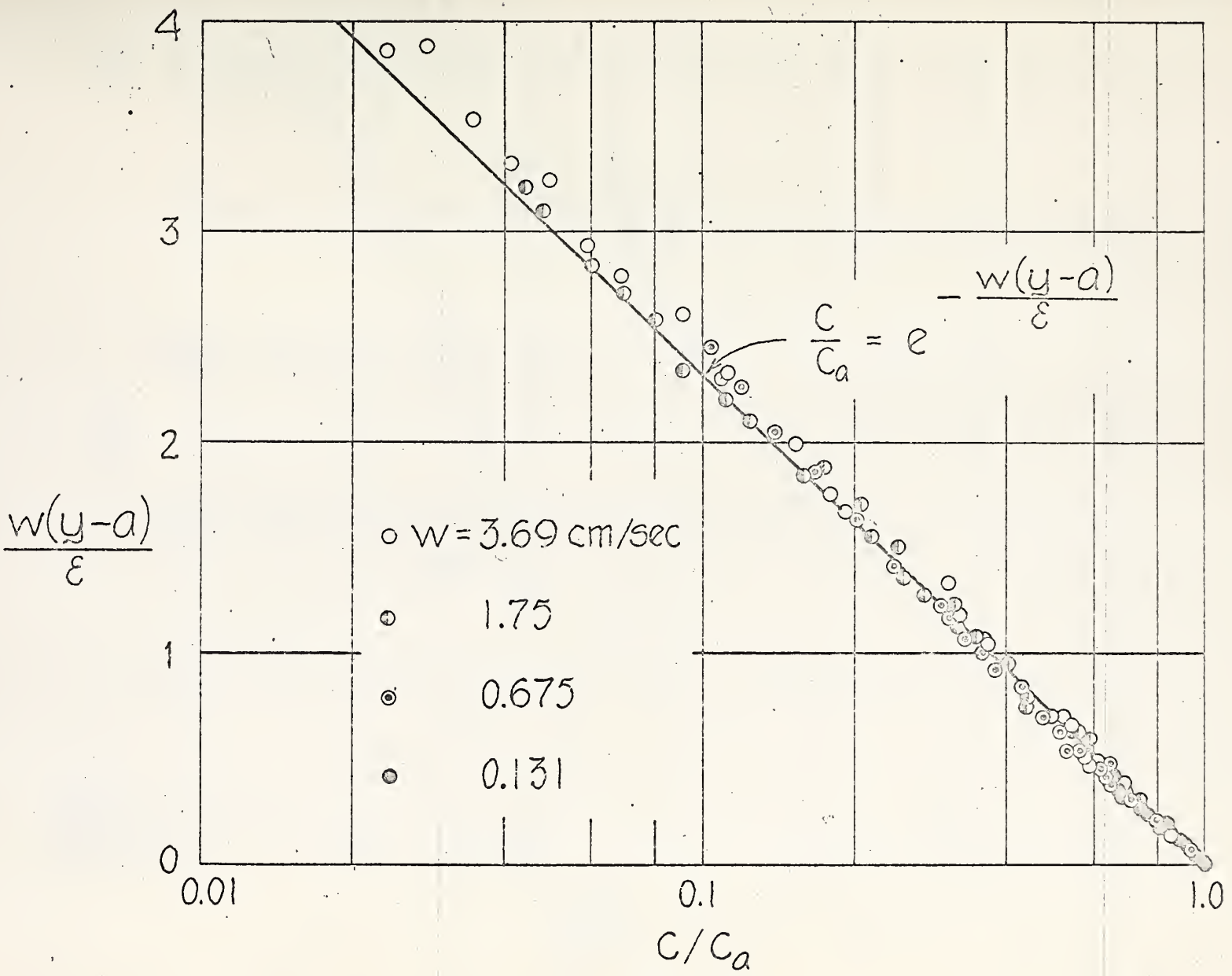

[31]

Fig. 7.
Experimental verification of the theory of sediment suspension.

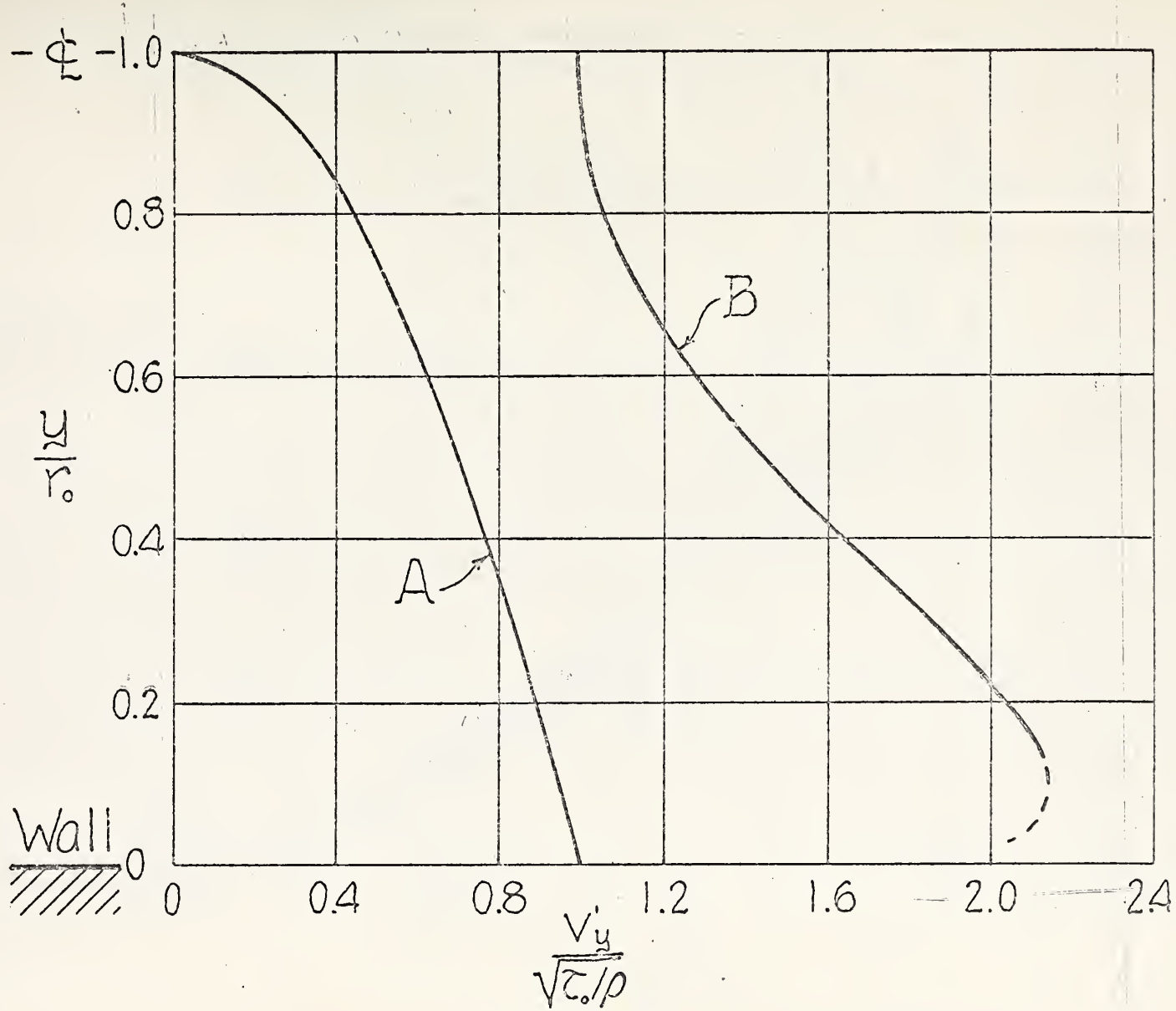

Fig. 9.

Variation of the radial component of velocity fluctuation across a pipe.

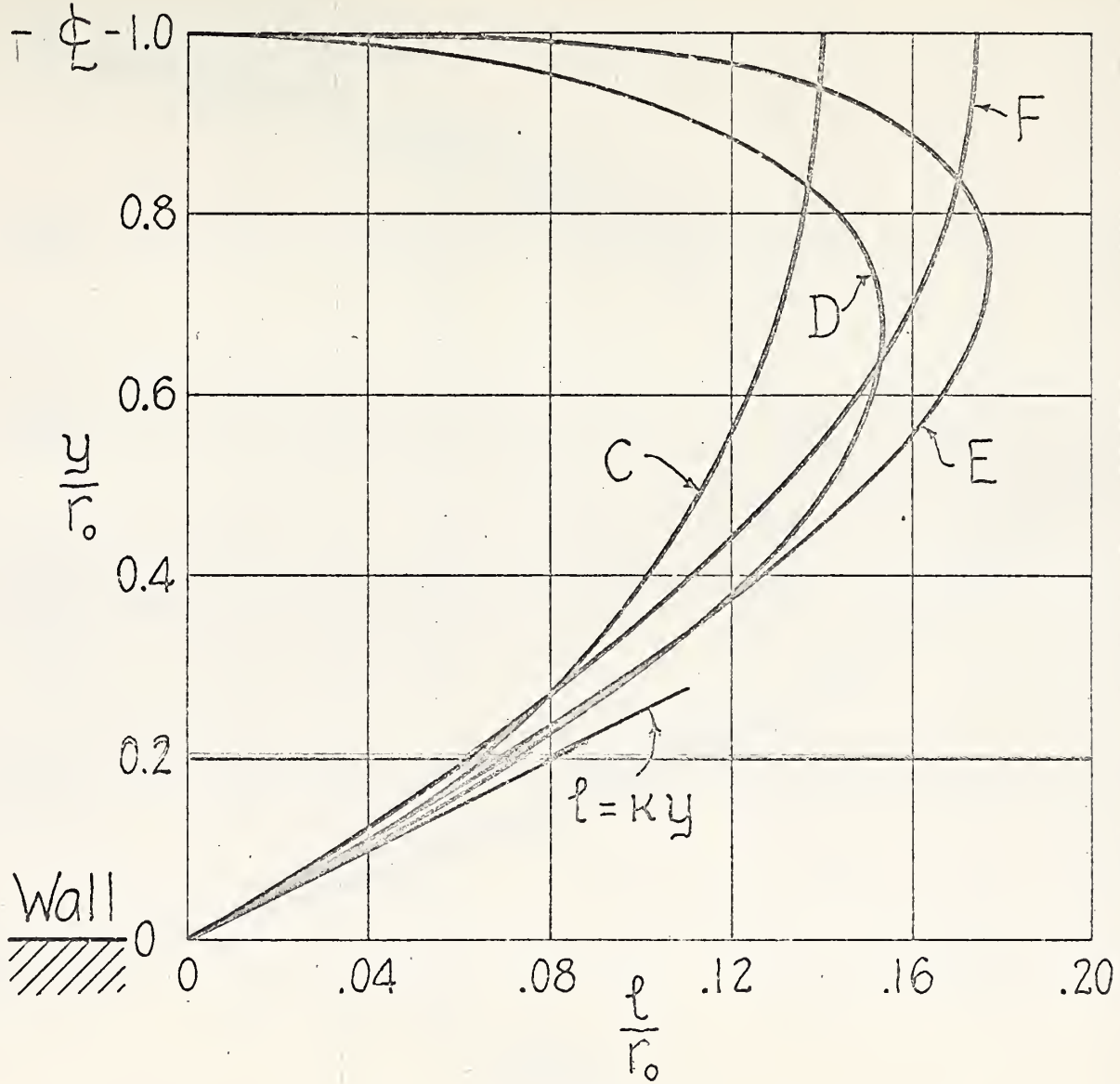

Fig. 10.

Variation of the length scale of turbulence across a pipe.

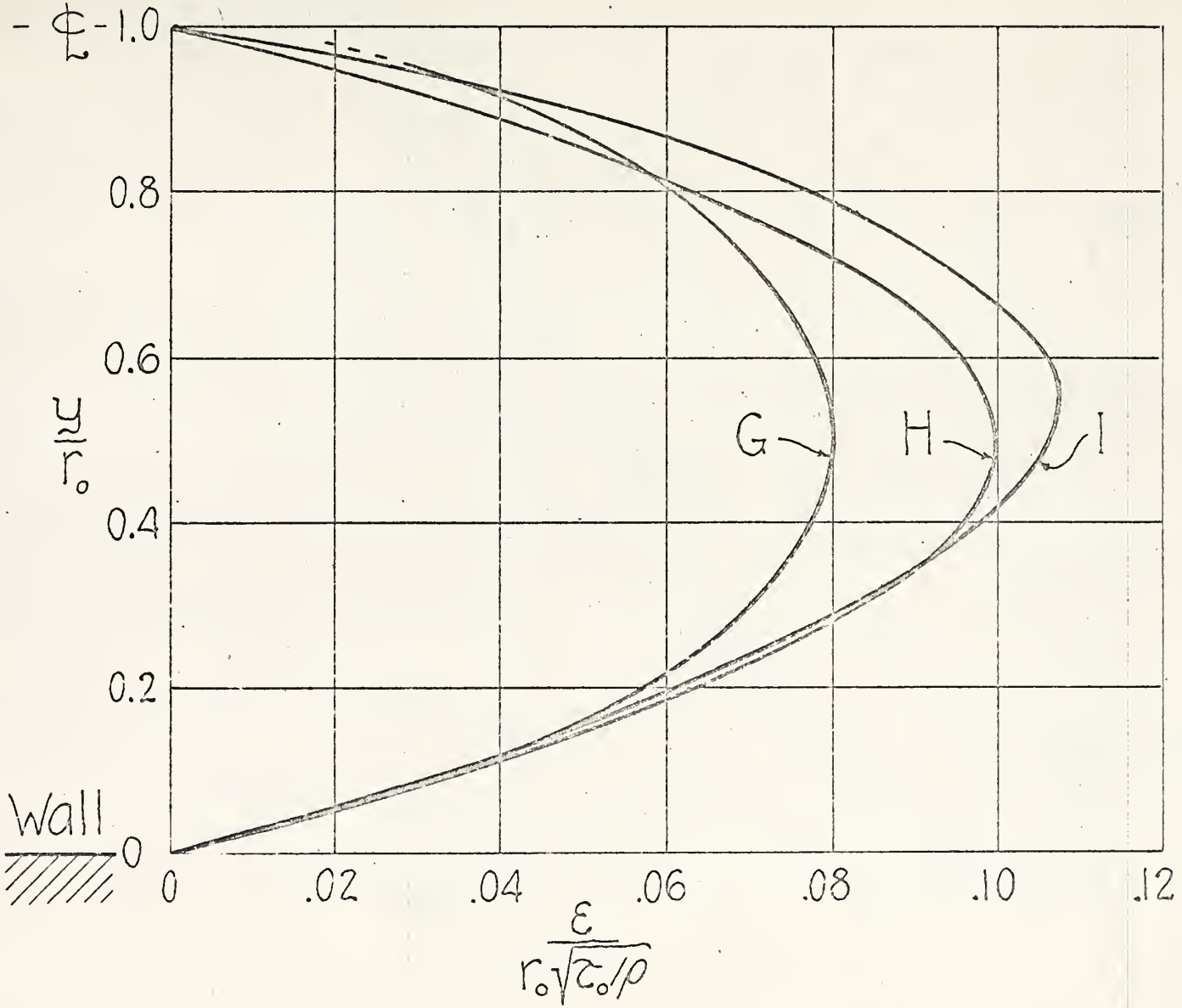

Fig. 11.

Variation of the coefficient of mixing across a pipe.

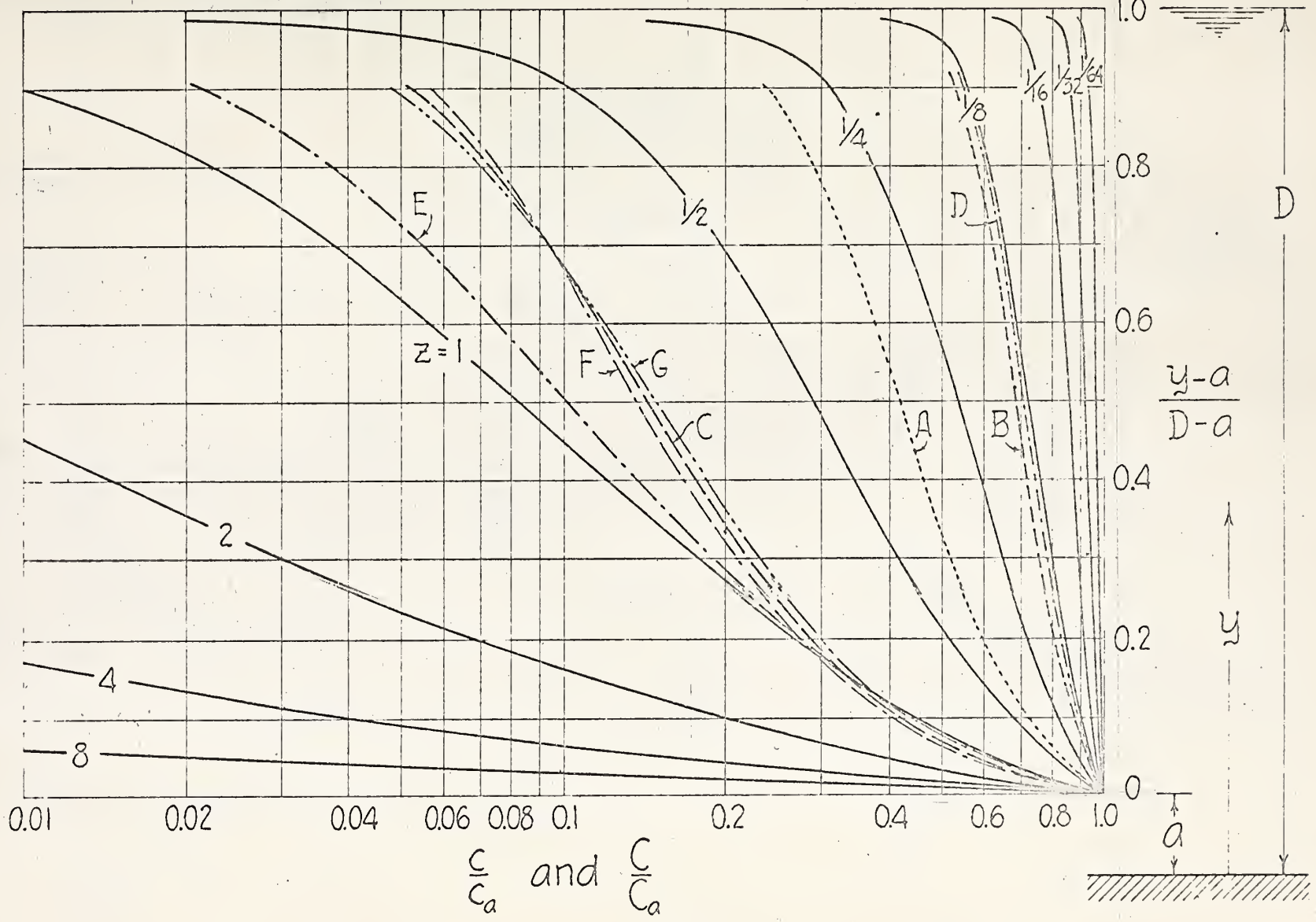

Fig. 12.

Distribution of suspended load in an open channel according to Equation (30).

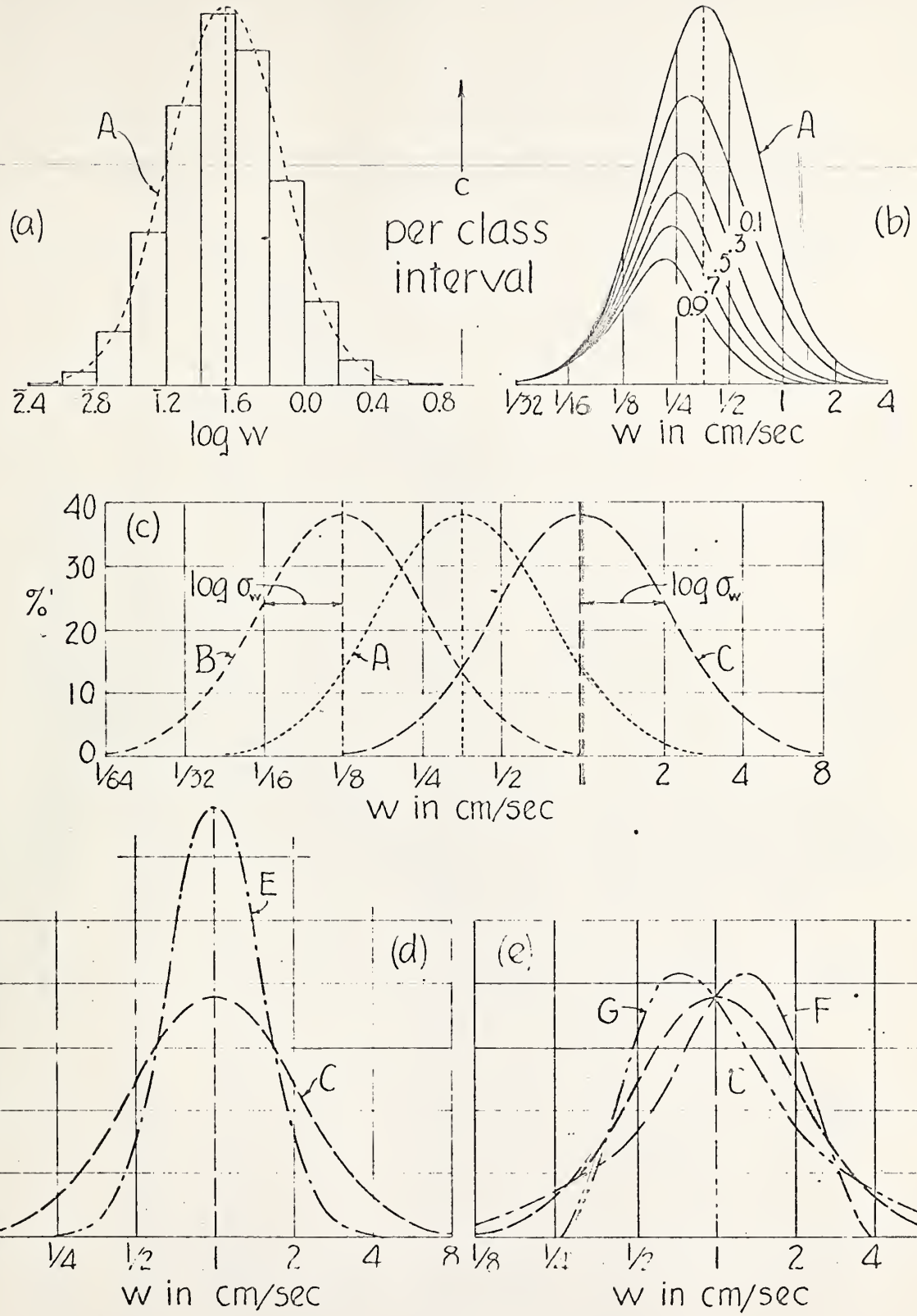

Fig. 13.
Definition sketches for the weight-frequency distribution of w .

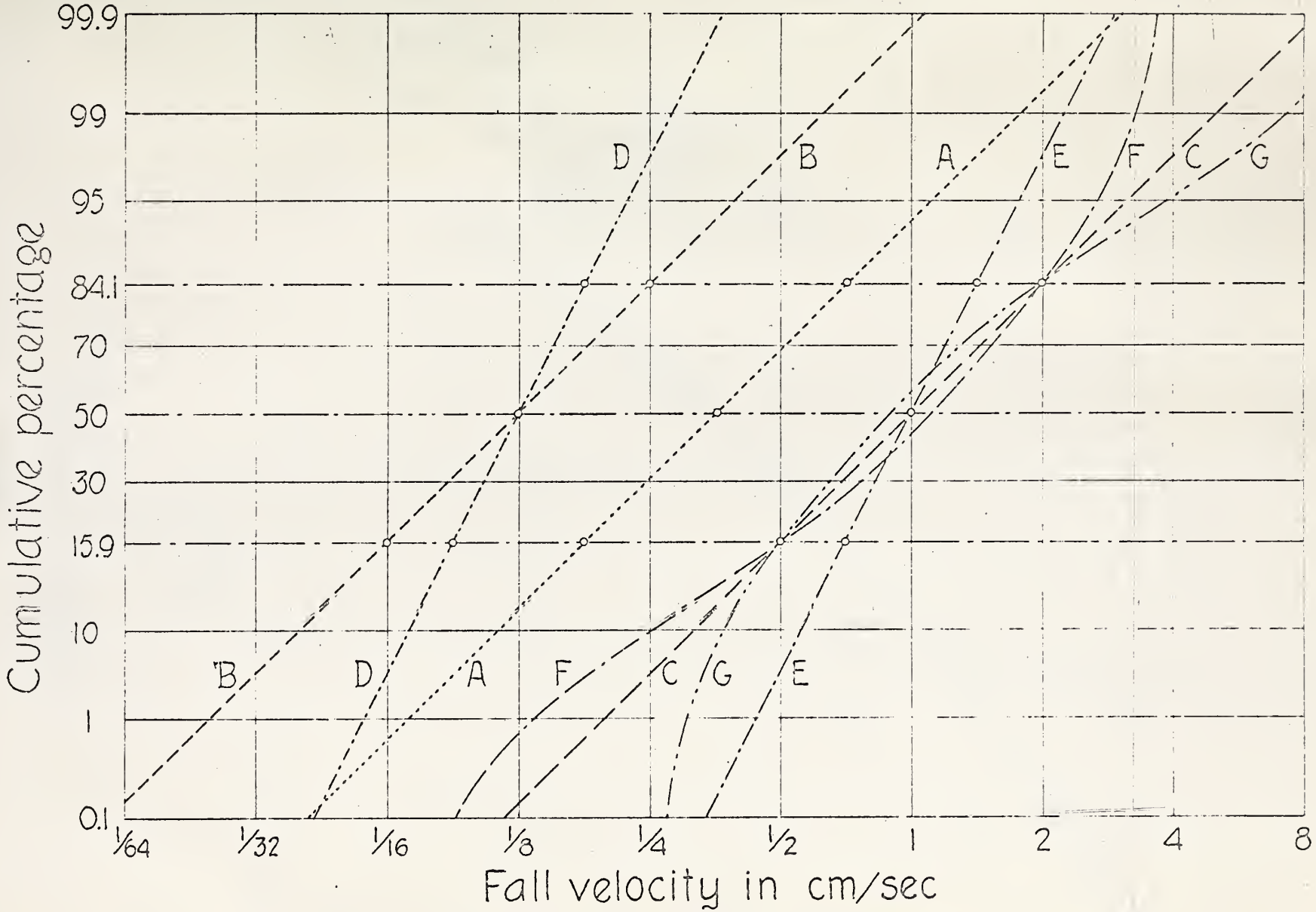

Fig. 14.

Cumulative logarithmic-probability plots corresponding to the frequency diagrams of Fig. 13.

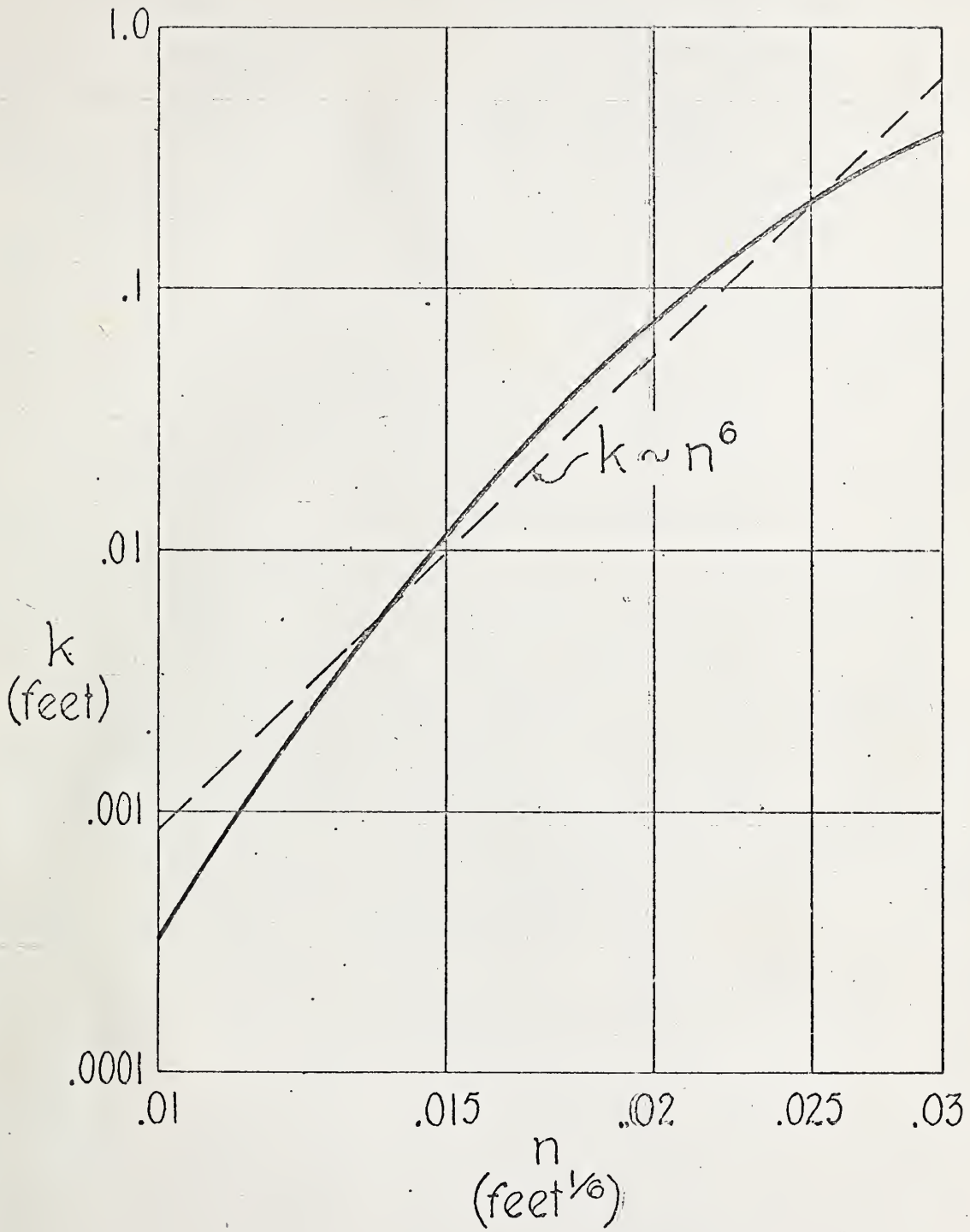

Fig. 15.

Absolute boundary roughness as a function of the Manning n .